Inorg. Chem. **2002**, *41*, 2341–2347

Magnetic Coupling and Intermetallic Electron Transfer in the Heterodinuclear Bioctahedral Complexes $MW^{III}Cl_9^{n-}$ ($M = V^{II}$, Cr^{III}, Mn^{IV}): Tweaking the Balance between Ferromagnetism and Antiferromagnetism

Simon Petrie and Robert Stranger*

Department of Chemistry, The Faculties, The Australian National University, Canberra ACT 0200, Australia

Received September 12, 2001

Density functional theory (DFT) calculations have been used to investigate the effect of intermetallic electron transfer on the mode of magnetic coupling in the face-shared bimetallic complexes $MWCl_9^{n-}$ (M = V, Cr, Mn; all with a nominal d^3 valence electronic configuration on each metal atom). These calculations illustrate a simple rule: when the oxidation state of M is lower than that of W, antiferromagnetic coupling is preferred, while ferromagnetism (via crossed exchange pathways) is favored when M has the higher oxidation state. This underlying trend in intermetallic interactions is seen to depend on the interplay among ligand field splitting, spin polarization splitting of α- and β-spin orbitals, and the relative energies of the M and W valence d orbitals, and is mirrored in the results seen in a wider survey of mixed-metal, face-shared complexes.

Introduction

Most laboratory studies of dinuclear transition-metal complexes to date have concerned the properties of homobimetallic complexes; investigations on complexes containing two disparate metal atoms are often hampered by significantly greater synthetic difficulties. There is, therefore, much which remains to be learned concerning the modes of intermetallic interaction in heterodinuclear transition-metal compounds. One rationale for the study of such complexes is the observation that many protein active sites are heterobimetallic: examples include the combination of Fe^{3+} with Ni^{2+} in NiFe hydrogenase,[1] Fe^{3+} with Cu^{2+} in cytochrome *c* oxidase,[2,3] and Fe^{3+} with Mn^{2+} in purple acid phosphatase.[4] In the biomolecules cited above, intermetallic separations are too large to support any metal−metal bonding, and consequently the interaction between metals is restricted to magnetic coupling.

Several recent studies have reported interesting variations in magnetic behavior in series of structurally related heterobinuclear complexes. Families of $Fe^{III}M^{II}$ (M = Mn, Co, and Ni),[5] $V^{IV}M^{II}$ (M = Mn, Fe, Co, Ni, and Cu),[6] and $Cu^{II}M^{II}$ (M = Mn, Fe, Ni, and Cu)[7] complexes have all been found to exhibit progressively stronger magnetic coupling as M moves across the first transition series; for the Fe^{III}- and V^{IV}-containing complexes,[5,6] the mode of coupling switches from antiferromagnetic to ferromagnetic beyond M = Mn, while the $Cu^{II}M^{II}$ complexes remain antiferromagnetic across the range of M^{II} ions surveyed.[7] B3-LYP hybrid DFT calculations on these $Cu^{II}M^{II}$ complexes also found them to be antiferromagnetic,[8] while calculations on two analogous $Cu^{II}M^{III}$ complexes (M = Cr, Mn) indicated a switch to ferromagnetic coupling.[8] Another theoretical study[9] of oxo-bridged complexes containing Ti^{III}/V^{III} and Ti^{III}/Cr^{III} has found these species to be ferromagnetically coupled, whereas the analogous V^{III}/Cr^{III} complex is antiferromagnetic. Such studies clearly show that the mode of magnetic coupling can be "tuned" by a judicious choice of the metal combination,

* To whom correspondence should be addressed. E-mail: rob.stranger@anu.edu.au.

(1) Volbeda, A.; Charon, M.-H.; Piras, C.; Hatchikian, E. C.; Frey, M.; Fontecilla-Camps, J. C. *Nature* **1995**, *373*, 580.
(2) Ferguson-Miller, S.; Babcock, G. T. *Chem. Rev.* **1996**, *96*, 2889.
(3) Michel, H.; Behr, J.; Harrenga, A.; Kannt, A. *Annu. Rev. Biophys. Biomol. Struct.* **1998**, *27*, 329.
(4) Schenk, G.; Boutchard, C. L.; Carrington, L. E.; Noble, C. J.; Moubaraki, B.; Murray, K. S.; de Jersey, J.; Hanson, G. R.; Hamilton, S. *J. Biol. Chem.* **2001**, *276*, 19084.
(5) Dutta, S. K.; Werner, R.; Flörke, U.; Mohanta, S.; Nanda, K. K.; Haase, W.; Nag, K. *Inorg. Chem.* **1996**, *35*, 2292.
(6) Mohanta, S.; Nanda, K. K.; Thompson, L. K.; Flörke, U.; Nag, K. *Inorg. Chem.* **1998**, *37*, 1465.
(7) Birkelbach, F.; Winter, M.; Flörke, U.; Haupt, H. J.; Butzlaff, C.; Lengen, M.; Bill, E.; Trautwein, A. X.; Wieghardt, K.; Chaudhuri, P. *Inorg. Chem.* **1994**, *33*, 3990.
(8) Cano, J.; Rodriguez-Fortea, A.; Alemany, P.; Alvarez, S.; Ruiz, E. *Chem.—Eur. J.* **2000**, *6*, 327.
(9) Kolczewski, C.; Fink, K.; Staemmler, V. *Int. J. Quantum Chem.* **2000**, *76*, 137.

10.1021/ic0109703 CCC: $22.00
Published on Web 03/30/2002

and it is tempting to infer that some such (metabolically effective) purpose is served by the juxtaposition of different transition metals within certain biomolecules. However, it seems that the bulk of the existing research on this topic has explored the influence of substituting different metal atoms *in the same charge state* rather than varying the metal atom identity *while conserving the number of d electrons*. We have chosen to take the latter approach in the present work, which describes a preliminary investigation into the interplay between intermetallic electron transfer and magnetic properties in weakly coupled heterodinuclear complexes.

Because few experimental data are yet available on this topic, it is essential that the theoretical methods employed are reliable and accurate. These criteria are well met by density functional theory, which has been shown (in a wide variety of previous studies)[10−14] to yield results of accuracy comparable to that of state-of-the-art ab initio quantum chemical calculations using coupled-cluster methods. It is important, also, that the model compounds studied are electronically well-behaved—that is, that the various modes of magnetic coupling and/or metal−metal bond formation can be represented by single-determinant wave functions. The d^3d^3 face-shared nonachloride complexes $MWCl_9^{n-}$ which we describe here fulfill this condition, and have the added virtues (while not in themselves the subject of any previous study) of being members of a series of compounds for which considerable experimental data already exist (for the homonuclear dimers $Cr_2Cl_9^{3-}$,[15−18] $Mo_2Cl_9^{3-}$,[19,20] $W_2Cl_9^{3-}$,[21−23] and $Re_2Cl_9^{-}$,[24−26] and the same-group dimer $CrMoCl_9^{3-}$),[27] and for which DFT calculations[28−32] have shown consistently good agreement with existing experimental observations. We would hope that, by extending the theoretical treatment of these face-shared binuclear complexes to mixed-group dimers such as $MnWCl_9^{2-}$, we can provide a valuable insight into the influence of metal−metal electron transfer on structural and magnetic trends in these and other bimetallic, mixed-group transition-metal complexes.

Computational Details

All calculations described in this work were performed on Linux-based Pentium III 600 MHz computers using the Amsterdam Density Functional (ADF) program, version ADF1999,[33] developed by Baerends et al.[34] All calculations employed the local density approximation (LDA) to the exchange potential,[35] and the correlation potential of Vosko, Wilk, and Nusair,[36] unless otherwise indicated. Scalar relativistic corrections, where specified, were obtained using the zero-order regular approximation (ZORA) formalism.[37] In relation to metal−metal distances, previous studies on chloride-bridged[30] and oxo-bridged[38] dimeric anions have shown that the LDA generally offers significantly better agreement with experimental geometries than more computationally demanding DFT calculations incorporating nonlocal corrections to the exchange potential. More recently, we have undertaken a comprehensive reevaluation of this issue for a wide variety of bridged and unbridged bimetallic complexes, to explore the consequences of new basis sets, and methods (including the ZORA treatment[37] for relativistic corrections, and the B-LYP nonlocal correction to the density functional)[39,40] not available at the time of our earlier study.[30] This further exploration (which will be reported elsewhere)[41] provides substantial support for our continued use[28−32,42,43] of the local density approximation without additional nonlocal corrections to obtain optimized geometries for bimetallic compounds.

Basis sets for all atoms were triple-ζ quality with Slater-type orbitals (type IV). Electrons in orbitals up to and including 2p {Cl}, 3p {V, Cr, Mn}, and 4f (but excluding 5s and 5p) {W} were treated in accordance with the frozen-core approximation. Optimized geometries were obtained using the gradient algorithm of Versluis and Ziegler.[44] Calculations for the $S = 0$, $S = 2$, and $S = 3$ associated states and broken-symmetry calculations (employing an asymmetry in the initial spin densities upon the two metal atoms)[45] were performed in a spin-unrestricted manner using C_{3v} symmetry unless otherwise indicated. Potential energy curves for all pertinent

(10) Eriksson, L. A.; Pettersson, L. G. M.; Siegbahn, P. E. M.; Wahlgren, U. *J. Chem. Phys.* **1995**, *102*, 872.
(11) Barone, V.; Adamo, C. *J. Phys. Chem.* **1996**, *100*, 2094.
(12) Torrent, M.; Gili, P.; Duran, M.; Sola, M. *J. Chem. Phys.* **1996**, *104*, 9499.
(13) Niu, S.; Hall, M. B. *Chem. Rev.* **2000**, *100*, 353.
(14) Hu, Z. M.; Boyd, R. J. *J. Chem. Phys.* **2000**, *113*, 9393.
(15) Wessel, G. J.; Ijdo, D. J. W. *Acta Crystallogr.* **1957**, *10*, 466.
(16) Cotton, F. A. *Rev. Pure Appl. Chem.* **1967**, *17*, 25.
(17) Saillant, R.; Wentworth, R. A. D. *Inorg. Chem.* **1968**, *7*, 1606−1611.
(18) Grey, I. E.; Smith, P. W. *Aust. J. Chem.* **1971**, *24*, 73−81.
(19) Saillant, R.; Jackson, R. B.; Streib, W.; Folting, K.; Wentworth, R. A. D. *Inorg. Chem.* **1971**, *10*, 1453.
(20) Stranger, R.; Smith, P. W.; Grey, I. E. *Inorg. Chem.* **1989**, *28*, 1271.
(21) Dunbar, K. R.; Pence, L. E. *Acta Crystallogr.* **1991**, *C47*, 23.
(22) Watson, W. H., Jr.; Waser, J. *Acta Crystallogr.* **1958**, *11*, 689.
(23) Stranger, R.; Grey, I. E.; Madsen, I. C.; Smith, P. W. *J. Solid State Chem.* **1987**, *69*, 162.
(24) Strubinger, S. K. D.; Sun, I. W.; Cleland, W. E., Jr.; Hussey, C. L. *Inorg. Chem.* **1990**, *29*, 4246.
(25) Heath, G. A.; Raptis, R. G. *Inorg. Chem.* **1991**, *30*, 4106.
(26) Heath, G. A.; McGrady, J. E.; Raptis, R. G.; Willis, A. C. *Inorg. Chem.* **1996**, *35*, 6838.
(27) Matson, M. S.; Wentworth, R. A. D. *Inorg. Chem.* **1976**, *15*, 2139−2144.
(28) Lovell, T.; McGrady, J. E.; Stranger, R.; Macgregor, S. A. *Inorg. Chem.* **1996**, *35*, 3079−3080.
(29) McGrady, J. E.; Lovell, T.; Stranger, R. *Inorg. Chem.* **1997**, *36*, 3242−3247.
(30) McGrady, J. E.; Stranger, R.; Lovell, T. *J. Phys. Chem. A* **1997**, *101*, 6265−6272.
(31) McGrady, J. E.; Stranger, R.; Lovell, T. *Inorg. Chem.* **1998**, *37*, 3802−3808.
(32) Stranger, R.; Turner, A.; Delfs, C. D. *Inorg. Chem.* **2001**, *40*, 4093.
(33) Baerends, E. J.; A Bérces; Bo, C.; Boerrigter, P. M.; Cavallo, L.; Deng, L.; Dickson, R. M.; Ellis, D. E.; Fan, L.; Fischer, T. H.; Fonseca Guerra, C.; van Gisbergen, S. J. A.; Groeneveld, J. A.; Gritsenko, O. V.; Harris, F. E.; van den Hoek, P.; Jacobsen, H.; van Kessel, G.; Kootstra, F.; van Lenthe, E.; Osinga, V. P.; Philipsen, P. H. T.; Post, D.; Pye, C.; Ravenek, W.; Ros, P.; Schipper, P. R. T.; Schreckenbach, G.; Snijders, J. G.; Sola, M.; Swerhone, D.; te Velde, G.; Vernooijs, P.; Versluis, L.; Visser, O.; van Wezenbeek, E.; Wiesenekker, G.; Wolff, S. K.; Woo, T. K.; Ziegler, T. ADF1999, 1999.
(34) Fonseca Guerra, C.; Snijders, J. G.; te Velde, G.; Baerends, E. J. *Theor. Chem. Acc.* **1998**, *99*, 391−403.
(35) Parr, R. G.; Yang, W. *Density Functional Theory of Atoms and Molecules*; Oxford University Press: New York, 1989.
(36) Vosko, S. H.; Wilk, L.; Nusair, M. *Can. J. Chem.* **1980**, *58*, 1200.
(37) van Lenthe, E.; Ehlers, A. E.; Baerends, E. J. *J. Chem. Phys.* **1999**, *110*, 8943.
(38) Bridgeman, A. J.; Cavigliasso, G. *J. Phys. Chem. A* **2001**, *105*, 7111.
(39) Lee, C.; Yang, W.; Parr, R. G. *Phys. Rev. B* **1988**, *37*, 785.
(40) Becke, A. D. *Phys. Rev. A* **1988**, *38*, 3098.
(41) Petrie, S.; Stranger, R. Manuscript in preparation.
(42) Stranger, R.; McGrady, J. E.; Lovell, T. *Inorg. Chem.* **1998**, *37*, 6795−6806.
(43) Lovell, T.; Stranger, R.; McGrady, J. E. *Inorg. Chem.* **2001**, *40*, 39−43.
(44) Versluis, L.; Ziegler, T. J. *J. Chem. Phys.* **1988**, *88*, 322−328.
(45) Noodleman, L.; Norman, J. G., Jr. *J. Chem. Phys.* **1979**, *70*, 4903−4906.

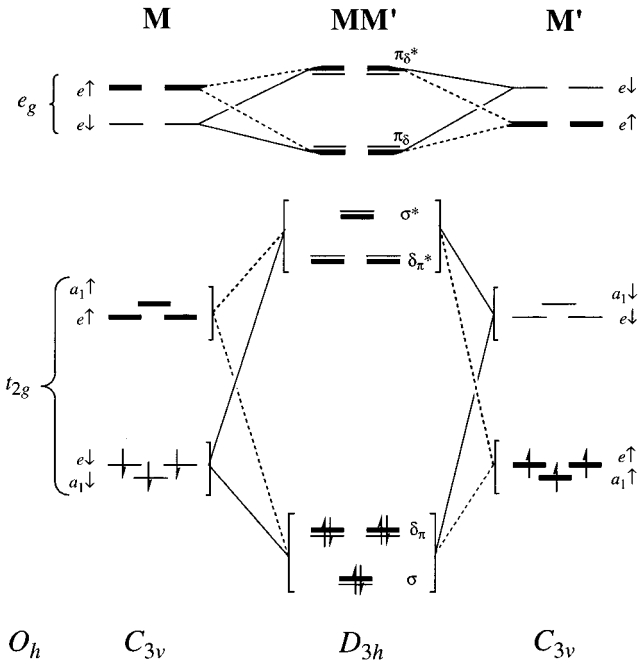

Figure 1. Representation of the $M_S = 0$ broken-symmetry state of a homonuclear dimer, $MM'Cl_9^{n-}$ (M = M′) in both localized and delocalized limits. Orbitals are labeled according to the representations of the C_{3v} point group.

states were obtained by optimization of all other structural parameters for the dimers along a series of fixed metal−metal separations.

Results and Discussion

Intermetallic Bonding and Electron Transfer: A Brief Overview. The valence d orbital diagram for a homonuclear face-shared dimer, $M_2X_9^{n-}$, shown in Figure 1, illustrates the lowest-energy electronic configurations expected (within the "broken-symmetry" constraint of $M_S = 0$, and C_{3v} symmetry) for both the nonbonded and triply bonded limiting cases. The t_{2g} orbitals of the "monomeric" octahedral complex are, in the dimer, split into symmetry-distinct subsets (depending upon their orientation relative to the intermetallic axis) of a_1 (σ) and e (δ_π) symmetry. The minima for the $S = 0$, $S = 2$, and $S = 3$ associated states correspond to, respectively, triple bond formation ($\sigma^2\delta_\pi^4$) with all valence d electrons delocalized between the two metals, single bond formation (σ^2) with the remaining four δ_π electrons weakly coupled (spin-aligned) within the t_{2g}-derived e orbital manifold, and nonbonding of all six, spin-aligned, valence d electrons within the a_1 and e orbitals in a weakly coupled complex. These orbital occupations are summarized in Figure 2. In a well-behaved dimer, the minima on the $S = 0$, $S = 2$, and $S = 3$ associated state surfaces are found at progressively increasing intermetallic separations, in accordance with expectations based upon the extent of metal−metal bonding as described above.

General Structural and Energetic Results. In Table 1, we present some key parameters calculated for the broken-symmetry state and for the various associated states of the $VWCl_9^{4-}$, $CrWCl_9^{3-}$, and $MnWCl_9^{2-}$ dimers. Except where otherwise specified, these values have been obtained from

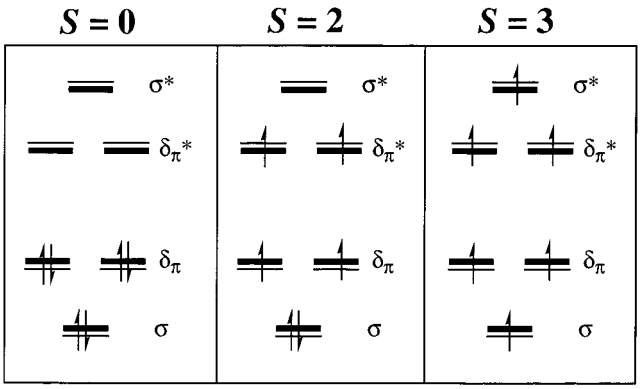

Figure 2. Representation of t_{2g}-derived orbital occupancy for the $S = 0$, $S = 2$, and $S = 3$ associated states for a generic dimer, $MM'Cl_9^{n-}$.

Table 1. Energetic and Structural Parameters for the Heterobimetallic Complexes $MWCl_9^{n-}$

parameter	$VWCl_9^{4-}$	$CrWCl_9^{3-}$	$MnWCl_9^{2-}$
$E_{rel}(S=0)^a$	0.336	0.749	0.308
$E_{rel}(S=2)^a$	0.193	0.253	−0.118
$E_{rel}(S=3)^a$	0.297	0.040	−0.315
$E_{tot}(BS)^b$	−43.1289	−50.9506	−53.5214
J^c	−270	−36	+280
$E_{rel}(S=3)/ZORA^{a,d}$	0.265	0.043	−0.417
$J/ZORA^{c,d}$	−240	−39	+370
$r_{S=0}(M-W)^e$	2.341	2.351	2.409
$r_{S=2}(M-W)^e$	2.918	2.861	3.250
$r_{S=3}(M-W)^e$	3.539	3.350	3.337
$r_{BS}(M-W)^e$	3.028	3.095	2.720
$S = 2$: $\rho_{spin}(M, W)^f$	2.15, 1.82	2.37, 1.53	3.94, −0.09
$S = 3$: $\rho_{spin}(M, W)^f$	2.94, 3.01	3.06, 2.76	3.89, 1.74
BS: $\rho_{spin}(M, W)^f$	2.53, −2.58	2.75, −2.71	2.22, −1.90

[a] Energy of the local minimum for the indicated associated state in electronvolts, expressed relative to the total bond energy of the broken-symmetry minimum. [b] Total bond energy of the BS minimum (eV). [c] Calculated magnetic exchange coupling constant (cm^{-1}). See the text for the definition. [d] The value shown for this parameter includes a scalar relativistic correction obtained using the ZORA formalism.[37] [e] Optimum M−W separation (Å) for the indicated associated state or BS state. [f] Covalency-corrected spin densities[51] on M and W, respectively, for the indicated associated state or BS minimum.

the geometry optimizations on each spin state, using the local density approximation with the VWN functional. For some parameters, we have also provided values obtained from single-point calculations incorporating a ZORA term for scalar relativistic effects.[37] Further values, obtained with the nonlocal B-LYP functional (both with and without ZORA corrections), were obtained but are not given here since we infer that they are less reliable than the VWN results for the properties of interest. A useful "test case" in this regard is the sole experimentally known heterodinuclear face-shared bioctahedron, $CrMoCl_9^{3-}$,[27,46] which we might reasonably expect to show very close structural, electronic, and magnetic similarities to the $CrWCl_9^{3-}$ dimer featured here. The $CrMoCl_9^{3-}$ complex has been found to exhibit moderate antiferromagnetic coupling in both the solid state and CH_2Cl_2 solution, with reported magnetic moments, per metal atom, of 2.19 μ_B (solid state, 300 K) and 2.27 μ_B (CH_2Cl_2 solution, 295 K).[27,46] Our VWN calculations on the BS and $S = 3$ configurations of $CrMoCl_9^{3-}$ yield $J = -24$ cm^{-1} (or

(46) Matson, M. S.; Wentworth, R. A. D. *J. Am. Chem. Soc.* **1974**, *96*, 7837.

-31 cm^{-1} with inclusion of a ZORA correction), while B-LYP single-point calculations using our VWN-optimized geometries yield $J = 62$ cm^{-1} (or 54 cm^{-1} with ZORA correction). These B-LYP results, even after consideration of mitigating effects,[47] are in clear conflict with the experimental observation of antiferromagnetic coupling. We conclude that, while use of nonlocal functionals such as B-LYP or B3-LYP may provide good performance in predicting magnetic properties in several classes of dinuclear complex,[48,49] this performance does not appear to extend to complexes in which the main mode of exchange is via direct metal−metal interaction (as in $CrMoCl_9^{3-}$) rather than by superexchange.

Several significant trends are apparent in the data given in Table 1.

First, the energy difference E_{rel} ($S = 3$), which represents the height of the $S = 3$ minimum above the corresponding broken-symmetry (BS) minimum, becomes progressively lower as M is stepped from V to Cr to Mn. The negative value for $MnWCl_9^{2-}$ indicates that ferromagnetic coupling is the preferred mode of intermetallic interaction in this dimer. The magnetic behavior of the complexes is denoted also by the magnetic exchange constant J ($H = -2JS_1S_2$), where J is calculated from the expression[50]

$$-2J = 2(E(S_{max}) - E_{BS})/S_{max}^2 \quad (1)$$

In the present case, where $S_{max} = 3$, this corresponds to the relationship $J = -E_{rel}(S = 3)/9$.

Second, for both $VWCl_9^{4-}$ and $CrWCl_9^{3-}$, the metal−metal elongation from the $S = 0$ to $S = 2$ to $S = 3$ minima is essentially regular: the optimum $S = 2$ "single bond" length is approximately intermediate between those of the $S = 0$ "triple bond" and $S = 3$ "nonbonded" minima. This is not the case for $MnWCl_9^{2-}$, where the $S = 2$ bond length is unusually large (and is, in fact, close to that of the $S = 3$ minimum).

Third, for both $VWCl_9^{4-}$ and $CrWCl_9^{3-}$, the optimum M−W distance from the BS calculation is somewhat larger than the corresponding $S = 2$ bond length, suggesting that the bonding interaction in these dimers is quite weak. This is borne out by the calculated covalency-corrected[51] spin densities for the BS minima, which suggest bond orders of $\sim 0.2-0.5$.[52] In contrast, the $MnWCl_9^{2-}$ BS minimum is notably short (severely so when assessed against the $MnWCl_9^{2-}$ $S = 2$ minimum, but obviously smaller also than the other singly bonded $S = 2$ minima). Perusal of the $MnWCl_9^{2-}$ BS spin densities suggests a bond order for this species of $\sim 0.9-1.0$.

Fourth, for the $S = 2$ and $S = 3$ associated states, an increasing anisotropic distribution of d electron spin density between the metals is apparent as M changes from V to Cr to Mn. For both associated states, nonbonding d electrons are localized equally on V and W, more on Cr than on W, and predominantly on Mn rather than W: in the most extreme case, essentially all of the localized electrons in the $MnWCl_9^{2-}$ $S = 2$ minimum are found on Mn.

All of the points noted above can satisfactorily be explained as arising from the interplay among spin-polarization splitting of the α- and β-spin orbitals, ligand-field splitting, and the mean relative energies of the valence d orbitals on M and W, as is perhaps most readily demonstrated in Figure 3. The purpose of this figure is to indicate, in a generalized fashion, the potentiality for M/W electron transfer in each of the various spin states for the M/W combinations. (Relative energy levels depicted in the figure are illustrative, and should not be construed as precise in all instances.) Splitting of the 3d valence orbitals on M is dominated by spin-polarization effects, while the more diffuse 5d orbitals on tungsten are largely split as a result of ligand-field effects. When this is coupled with the general stabilization of d orbitals with higher oxidation state, we can satisfactorily rationalize the results obtained for each M/W combination.

For $VWCl_9^{4-}$, opportunities for V → W electron transfer are much greater for the BS and $S = 2$ states than for $S = 3$. A d^3d^3 occupation in either the BS or $S = 2$ configuration features vacant low-lying α-spin orbitals on W, whereas $S = 3$ lacks this feature. Antiferromagnetic coupling (BS), in association with α-spin $t_{2g}(V) \rightarrow t_{2g}(W)$ electron transfer predominantly involving the favorably oriented σ-symmetry (a_1) metal atom d orbitals, is therefore preferred over ferromagnetism ($S = 3$). However, any α-spin electron donation from V to W serves to destabilize the remaining α-spin occupation of V-localized orbitals, by diminishing

(47) One caveat which might be offered regarding the B-LYP single-point values is that B-LYP exhibits an innate preference for localization of d electrons on metal atoms, disfavoring metal−metal bonding. In our VWN geometry optimizations, the degree of metal−metal bonding in the BS minimum, which has a Cr−Mo separation of 3.20 Å, is clearly higher than that in the $S = 3$ minimum (r(Cr−Mo) = 3.33 Å), and this may act to additionally destabilize the BS geometry in the B-LYP single-point calculations. Evidence which supports this is that the B-LYP-optimized geometry on the BS configuration has a markedly longer Cr−Mo distance (3.51 Å). Use of B-LYP-optimized geometries does offer some improvement over the combination of B-LYP single-point energies and VWN geometries, but the B-LYP-optimized coupling constants ($J = 6$ cm^{-1}, or 7 cm^{-1} after ZORA correction) still indicate an erroneous preference for ferromagnetic coupling for this complex.

(48) Ruiz, E.; Alemany, P.; Alvarez, S.; Cano, J. *J. Am. Chem. Soc.* **1997**, *119*, 1297.

(49) Ruiz, E.; Cano, J.; Alvarez, S.; Alemany, P. *J. Comput. Chem.* **1999**, *20*, 1391.

(50) Noodleman, L. *J. Chem. Phys.* **1981**, *74*, 5737−5743.

(51) The raw Mulliken spin densities were corrected by a factor of $3/\rho_{M(oct)}$, where $\rho_{M(oct)}$ is the Mulliken spin density obtained for the central metal atom within the isolated high-spin d^3 octahedral complex MCl_6^{n-}. The purpose of this correction factor is to allow for the effect of M−Cl bond covalency within the octahedral complex: covalency reduces the spin density from the value of 3 expected for a purely ionic complex featuring a d^3 metal atom. We assume for simplicity that the extent of M−Cl bond covalency within the mixed-group dimer is similar to that found for the octahedral complex. This assumption ignores the distorting effect of electron transfer between the two metal atoms within the dimer, but we have previously found that this assumption holds very well within same-group dimers, and within a larger set of mixed-group dimers, the sum of the adjusted ρ_M and $\rho_{M'}$ values is always within ±5% of the values of 4.0 and 6.0 expected for the $S = 2$ and $S = 3$ associated states, respectively. We conclude that the "covalency correction" to the spin densities is essentially appropriate for the mixed-group dimers.

(52) The bond orders are obtained as the value $3.0 - \rho_{spin}$(BS), where the BS spin density on each metal is taken to represent the localized d electron content, and the difference from the expected total of 3 electrons per metal indicates the delocalized, or M−W bonding, content.

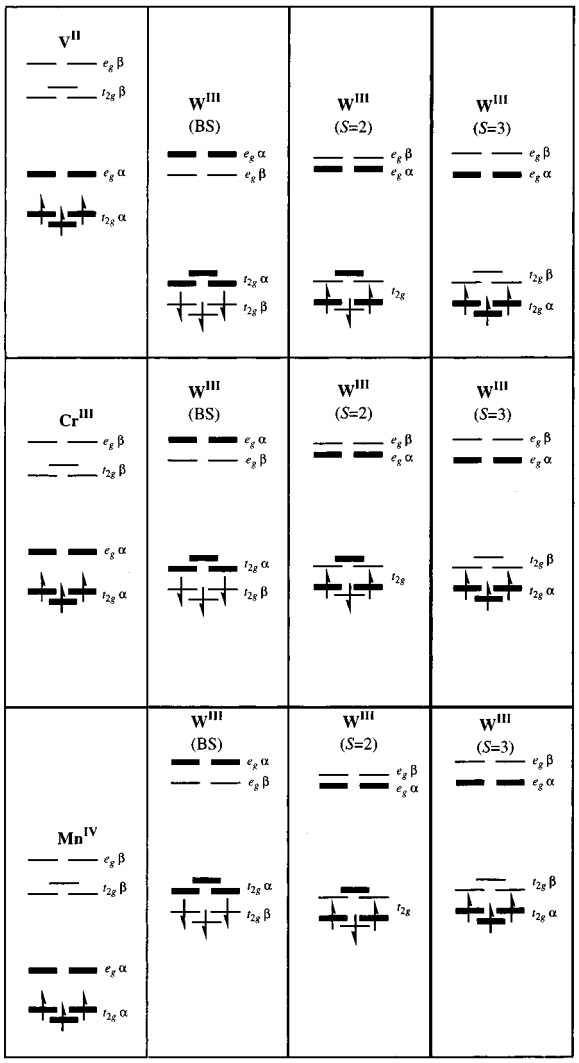

Figure 3. Stylized atomic energy level diagrams for V(II), Cr(III), Mn(IV), and W(III), as expected in a weakly coupled heteronuclear dimer. For convenience, we adopt the convention that the spin excess on the first-row metal is always α-spin. Assignment of the initial spin density on the first-row metal as 3, and on W as 1, in the weakly coupled limit for the $S = 2$ configuration is consistent with the relative magnitudes of spin-polarization splitting of α- and β-spin orbitals for first- and third-row d^3 transition-metal ions. Opportunities for intermetallic electron transfer, resulting in distortion from the "pure" d^3d^3 valence electronic configurations shown here, exist when a vacant orbital of the appropriate spin (α, thick lines; β, thin lines) and symmetry lies below a filled orbital on the other metal. DFT calculations show how the direction of intermetallic electron transfer, in face-shared (nominally d^3d^3) binuclear complexes of the formula $MWCl_9^{n-}$ (M = V, Cr, Mn), has a profound influence on the preferred mode of magnetic coupling. For example, the W → Mn electron transfer depicted here is found to promote strong ferromagnetic coupling, whereas antiferromagnetic coupling is favored by W ← V electron transfer.

the extent of spin-polarization splitting on V, and therefore the preference for antiferromagnetic coupling is not great.

For $CrWCl_9^{3-}$, the prospects for Cr ↔ W electron transfer are limited. Mixing of the filled α-spin t_{2g}-based orbitals on Cr with the corresponding (and low-lying) vacant α-spin orbitals on W in the BS and $S = 2$ configurations, might be expected to favor Cr → W electron transfer in these configurations, to a small extent, while the $S = 3$ configuration permits mixing of the (vacant) Cr e_g and (filled) W t_{2g} e-symmetry α-spin orbitals, i.e., a net W → Cr electron transfer. However, analysis of the filled molecular orbital (MO) composition for each of these configurations does not indicate any significant electron transfer between metals. On balance, expected orbital energetics do not significantly favor one mode of magnetic coupling over the other, and this is in accord with the results of our calculations. It appears that $CrWCl_9^{3-}$ (for which an attempted synthesis was unsuccessful)[27] is very similar, in terms of both structural and magnetic propeties, to $CrMoCl_9^{3-}$:[27,46] both complexes are significantly antiferromagnetic, albeit less strongly so than $Mo_2Cl_9^{3-}$.[19,20,53]

For $MnWCl_9^{2-}$, the energetic benefits of α-spin t_{2g} → e_g W → Mn electron transfer (for the $S = 2$ and $S = 3$ configurations) are clearly much greater than for β-spin W/Mn mixing (which again corresponds to a mode of W → Mn electron transfer) for the BS configuration.[54] The consequent additional stabilization of the $S = 2$ and $S = 3$ configurations by this electron transfer is thus able to account for our observation that these associated states lie lower in energy than the BS minimum. Note, also, that α-spin electron transfer from W to Mn serves to further increase the spin-

(53) Saillant, R.; Wentworth, R. A. D. *Inorg. Chem.* **1969**, *8*, 1226.

(54) A more detailed analysis of the electronic configuration of the $MnWCl_9^{2-}$ dimer in its various spin states involves elucidation of the metal atomic orbital (AO) contributions to the occupied valence d molecular orbitals (MOs). Perusal of the MO composition for the BS configuration reveals that the e-symmetry valence MOs are localized almost entirely on Mn (α) or displaying a modest amount of W → Mn leakage (β). The a_1-symmetry MOs for this configuration, which correspond closely to a linear combination of the M and W d_{z2} atomic orbitals, are comprised almost entirely of Mn content (α) or almost an equal admixture of Mn and W AOs (β). Since no Mn−W α-spin electron transfer is evident in any of these orbital descriptions, we can categorize the covalency-corrected spin density for W as accurately representing the residual d electron count on tungsten: that is, a nominal value of approximately 2 d electrons, with the loss of d electron density resulting almost equally from delocalization of the a_1-symmetry β-spin orbital (corresponding to partial Mn−W σ-bond formation) and from β-spin W (t_{2g})/Mn (e_g) e-symmetry MO mixing. In contrast, the MO composition for the $S = 3$ configuration, in which all d electrons are α-spin, shows complete localization of the a_1-symmetry orbitals on Mn ($12a_1$) and on W ($13a_1$), with the lower-energy valence d e-symmetry MO pair (14e) also localized purely on Mn. The highest occupied e-symmetry MO pair (15e) shows strong mixing (~50:50) between W (t_{2g}) and Mn (e_g) content. Thus, this configuration also features donation of approximately 1 electron from W to Mn. It is instructive to contrast the tendency toward electron transfer (approximately equal for the BS and $S = 3$ minima) with the relative stability of different spin states ($S = 3$ greatly favored over BS). As discussed in the text, this is directly attributable to the relative extent of spin-polarization stabilization possible in the low-spin (BS) and high-spin ($S = 3$) scenarios. The breakdown of BS state W → Mn electron transfer into β-spin a_1-mediated (Mn−W bonding) and e-mediated (W → Mn mixing) components would be expected to result in a reduction in the tendency for W → Mn electron transfer on the BS surface at larger Mn−W distances. This is precisely what is seen in the results of partial geometry optimizations for the BS and $S = 3$ states with r(Mn−W) constrained at a value of 3.6 Å, i.e., too great a separation for any significant metal−metal bonding interactions. For the 3.6 Å partially optimized BS geometry, we obtain covalency-corrected ρ_{spin} values of 2.42 and −2.30 on Mn and W, respectively, corresponding to net transfer of only about 0.6−0.7 electron: this corresponds very closely to the reduced degree of Mn d_{z2} AO content in the β-spin a_1-symmetry valence *d* MO. In contrast, the degree of electron transfer evident for the $S = 3$ 3.6 Å partially optimized geometry is actually increased slightly compared to its optimized value: corrected ρ_{spin} values here are 4.08 and 1.57 for Mn and W, respectively. Thus, the α-spin e-symmetry orbital mixing implicated in the $S = 3$ electron transfer is not apparently adversely affected by this increase in the metal−metal separation. Our 3.6 Å separation calculations also suggest that the existence of a bonding interaction between Mn and W in the BS configuration acts to significantly mitigate the BS/$S = 3$ energy gap: for the 3.6 Å geometries, this BS/$S = 3$ gap is increased to a value of 0.59 eV.

polarization splitting on Mn, which may be contrasted with the decrease in spin-polarization splitting on V → W electron transfer as discussed above. This synergistic interplay between Mn spin polarization and the Mn/W orbital energy levels strengthens the marked preference for ferromagnetic, rather than antiferromagnetic, coupling in this system. The mechanism of ferromagnetic coupling evident in $MnWCl_9^{2-}$ is an apparent example of "crossed exchange" [55−58] arising from strong overlap between a half-filled (W t_{2g}-based e-symmetry) and an empty (Mn e_g) α-spin orbital manifold. Such interactions have been widely noted to influence the magnetic character (whether by promoting ferromagnetic coupling or by weakening the overriding antiferromagnetic coupling) in a variety of dinuclear and polynuclear complexes.[58−62] While the strength of the ferromagnetic interaction in $MnWCl_9^{2-}$ is very strong, our value of $J = 280$ cm^{-1} (or 370 cm^{-1} after ZORA correction) does not appear exceptional: a value of $J = 200$ cm^{-1} has been obtained for a d^2d^2 μ-oxobis(μ-acetato)-bridged divanadium complex,[63] while $J > 200$ cm^{-1} has been determined for another d^2d^2 vanadium dimer featuring an oxo bridge.[58] The key feature in promoting ferromagnetism in these literature examples is the dominance of exchange between half-filled and vacant t_{2g}-based orbitals. Our calculations on $MnWCl_9^{2-}$ indicate a ferromagnetic pathway which differs in detail (that is, a difference in oxidation number and favorable orbital energies conspire to promote strong mixing between half-filled (t_{2g}-based) and vacant (e_g) orbitals) but which can satisfactorily be rationalized by a mechanism broadly similar to that operating in the ferromagnetic divanadium(III) complexes.[58]

The effect of the scalar relativistic corrections on our calculated magnetic exchange constants is also worth comment. It is noticeable that in the two complexes characterized by significant electron transfer, viz., $VWCl_9^{4-}$ and $MnWCl_9^{2-}$, the ZORA correction results in a greater degree of ferromagnetic character as indicated by the reduced J value, while the exchange constant for $CrWCl_9^{3-}$ is essentially unaffected. A consistent explanation for this behavior is that the relativistic correction serves to destabilize the tungsten d orbitals relative to those of the first-row metal. For $VWCl_9^{4-}$, this reduces the driving force for V → W electron transfer, thereby diminishing the stabilization of the BS minimum relative to $S = 3$. Conversely, for $MnWCl_9^{2-}$, the driving force for W → Mn electron transfer becomes further enhanced, particularly stabilizing the $S = 3$ minimum and thereby abetting ferromagnetic exchange in this dimer.

Preliminary calculations on other mixed-group face-shared (and nominally d^3d^3) $MM'Cl_9^{n-}$ complexes (which will be reported in detail elsewhere)[64] show that the salient factors noted above are applicable to all such complexes featuring a combination of M and M′ from groups V, VI, and VII. As exemplified in the results reported here for $MnWCl_9^{2-}$, ferromagnetism is found to be favored in these complexes *only* when the metal atom with the higher group number (which, if a d^3d^3 valence electron configuration is assumed, is the metal atom with the higher nominal oxidation number) is from the first transition series. Furthermore, the preference for ferromagnetic coupling over antiferromagnetic coupling is always most pronounced when the other metal atom is from the second or third transition series. Antiferromagnetic coupling occurs in competition with metal−metal bond formation when a first-transition-row metal atom is combined with a second- or third-transition-row metal from a higher group, as noted here for $VWCl_9^{4-}$. Neither ferromagnetic nor antiferromagnetic coupling is particularly favored when the dimer contains a first-row and a second- or third-row transition metal from the same group, as typified by $CrWCl_9^{3-}$. In all cases, these results can be satisfactorily interpreted in terms of a model such as that embodied in Figure 3. In such a model, the relative mean energies of the valence d orbital manifolds indicate the general tendency for electron transfer between M and M′, while the identities of M and M′ (as first-row or otherwise) indicate the preference for antiferromagnetic vs ferromagnetic coupling when discrete metal−metal bonding does not occur. It should also be noted that characterization of the energy differences between BS and $S = 3$ configurations as exchange splittings is not strictly correct: in the instances described here, these energetic splittings are for complexes with rather disparate distributions of the valence d electrons due to the greater preference for electron transfer in some spin states.

The factors outlined above will also be influential (in some manner) in determining the magnetic coupling mode in other mixed-group binuclear complexes, though the d^3d^3 complexes are arguably something of a "special case" for two reasons. First, when intermetallic electron transfer is ignored, each metal atom in a d^3d^3 dimer has a half-filled t_{2g}-based orbital subshell, and this significantly simplifies the resulting electronic structure of the complex: dimers having other d orbital configurations may not be adequately represented by single-determinant wave functions. Second, occupation of only the t_{2g}-based valence d orbitals ensures that the interaction between metals is predominantly direct, and is not greatly influenced by superexchange via the bridging ligands. Further studies are currently underway to elucidate the influence of intermetallic electron transfer on magnetic coupling tendencies in other combinations of valence electronic configurations, such as d^3d^5 and d^5d^6.

Concluding Remarks

Our density functional theory study of the mixed-group face-shared nonachlorides of groups V, VI, and VII reveals

(55) Goodenough, J. B. *Magnetism and the Chemical Bond*; Interscience: New York, 1963.
(56) Ginsberg, A. P. *Inorg. Chim. Acta* **1971**, 45.
(57) Blondin, G.; Girerd, J.-J. *Chem. Rev.* **1990**, *90*, 1359.
(58) Hotzelmann, R.; Wieghardt, K.; Flörke, U.; Haupt, H. J.; Weatherburn, D. C.; Bonvoisin, J.; Blondin, G.; Girerd, J.-J. *J. Am. Chem. Soc.* **1992**, *114*, 1681.
(59) Corbella, M.; Costa, R.; Ribas, J.; Fries, P. H.; Latour, J.-M.; Öhrström, L.; Solans, X.; Rodriguez, V. *Inorg. Chem.* **1996**, *35*, 1857.
(60) Weihe, H.; Güdel, H. U. *J. Am. Chem. Soc.* **1998**, *120*, 2870.
(61) Brunold, T. C.; Gamelin, D. R.; Solomon, E. I. *J. Am. Chem. Soc.* **2000**, *122*, 8511.
(62) Delfs, C. D.; Stranger, R. *Inorg. Chem.* **2001**, *40*, 3061.
(63) Brand, S. G.; Edelstein, N.; Hawkins, C. J.; Shalimoff, G.; Snow, M. R.; Tiekink, E. R. T. *Inorg. Chem.* **1990**, *29*, 434.
(64) Petrie, S.; Stranger, R. *Polyhedron*, submitted for publication.

a simple rule: the mode of magnetic coupling in a heterobinuclear, nominally d^3d^3 complex, $MM'Cl_9^{n-}$, lacking a direct metal−metal bond is influenced by the oxidation states and the row numbers of the constituent metals. For M = a first-row metal and M′ = a second- or third-row metal, antiferromagnetic coupling is favored when the oxidation state of M is lower than that of M′, while ferromagnetic coupling (via a crossed exchange mechanism, involving spin-specific electron transfer to the first-row metal's vacant e_g orbitals) is preferred when M has the higher oxidation state. When M and M′ have the same oxidation state, the preference for either mode of coupling is very slight. These trends can be rationalized in terms of the relative magnitudes of spin-polarization splitting and ligand-field splitting on the "electron-transfer acceptor", which is generally the more highly oxidized metal. While the preliminary results of our calculations on other d^3d^3 mixed-group, face-shared dimers are very encouraging, it remains to be seen whether this principle can be more widely applied toward a general understanding of magnetic coupling in mixed-metal dinuclear or oligonuclear complexes.

Acknowledgment. We gratefully acknowledge the Australian Research Council (ARC) for financial support.

IC0109703